Initial 3D Non-Linear Toroidal Results from the M3D-C^1 Code

Stephen C. Jardin[1]
N.M. Ferraro[2,3], J. Chen[1], J. Breslau[1], T. Scaffidi[1,4]

[1]*Princeton Plasma Physics Laboratory*
[2] *General Atomics*
[3]*Oak Ridge Institute for Science and Education, Oak Ridge TN*
[4]*École Normale Supérieure, Paris, France*

CEMM Meeting

Austin Texas
May 1, 2011

This work was performed in close collaboration with M. Shephard, F. Zhang, and F. Delalondre at the SCOREC center at Rensselaer Polytechnic Institute in Troy, NY.

PPPL PRINCETON PLASMA PHYSICS LABORATORY

Two Implicit Time-Advance Algorithms are being evaluated

Split θ-implicit Method

$$\left\{\rho-\theta^2(\delta t)^2 L\right\}\mathbf{V}^{n+1}=\left\{\rho-\theta(\theta-1)(\delta t)^2 L\right\}\mathbf{V}^{n}+\delta t\left\{-\nabla p+\frac{1}{\mu_0}(\nabla\times\mathbf{B})\times\mathbf{B}\right\}^{n}$$

Differential Approximation – DA (Caramana Method)

$$\left\{\rho-\theta^2(\delta t)^2 L\right\}\mathbf{V}^{n+1}=\left\{\rho-\theta^2(\delta t)^2 L\right\}\mathbf{V}^{n}+\delta t\left\{-\nabla p+\frac{1}{\mu_0}(\nabla\times\mathbf{B})\times\mathbf{B}\right\}^{n+1/2}$$

note!

MHD Operator: ⟶

$$L\{\mathbf{V}\}=\frac{1}{\mu_0}\left\{\nabla\times\left[\nabla\times\left(\mathbf{V}\times\mathbf{B}\right)\right]\right\}\times\mathbf{B}+\frac{1}{\mu_0}\left(\nabla\times\mathbf{B}\right)\times\left[\nabla\times\left(\mathbf{V}\times\mathbf{B}\right)\right]$$
$$+\nabla\left(\mathbf{V}\bullet\nabla p+\gamma p\nabla\bullet\mathbf{V}\right)$$

3D finite elements are constructed with a Reduced Quintic in (R,Z) and with a Hermite Cubic in φ

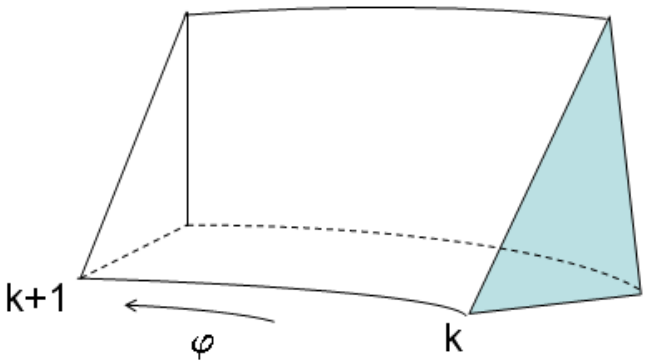

Each toroidal plane has two Hermite cubic functions associated with it

$$\Phi_1(x) = \left(|x|-1\right)^2\left(2|x|+1\right); \qquad \Phi_2(x) = x\left(|x|-1\right)^2$$

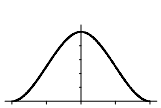

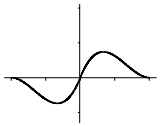

Solution for each scalar function is represented in each triangular wedge as the product of Q_{18} and Hermite functions.

- **Unstructured in (R,Z)**
- **Structured in φ**

$$U(R,Z,\varphi) = \sum_{j=1}^{18} \nu_j(R,Z)\Big[U^1_{j,k}\,\Phi_1(\varphi/h) + U^2_{j,k}\Phi_2(\varphi/h) + U^1_{j,k+1}\Phi_1(\varphi/h-1) + U^2_{j,k+1}\Phi_2(\varphi/h-1)\Big]$$

Continuous first derivatives in all directions and all DOF are located at nodes: => very efficient representation

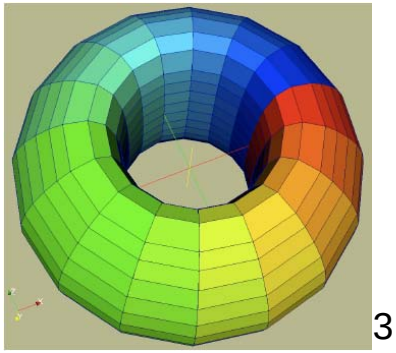

Linear and Non-linear modes in same code

Linear Mode

- All variables complex

$$\sim e^{in\varphi} \qquad \frac{\partial}{\partial \varphi} \rightarrow in$$

- Single 2D plane

$$\mathbf{A}_{2D} \bullet \mathbf{X}^{n+1} = \mathbf{B}_{2D} \bullet \mathbf{X}^{n}$$

- Factor $\mathbf{A}_{2D}$ once: $\mathbf{A}_{2D} = \mathbf{L} \bullet \mathbf{U}$
- Each time-step only involves matrix-vector multiply and back-substitution
- Very efficient

Non-Linear Mode

- All variables real
- Hermite cubic finite elements in φ
- Many 2D planes (P)

$$\mathbf{A}_{3D} \bullet \mathbf{X}^{n+1} = \mathbf{B}_{3D} \bullet \mathbf{X}^{n}$$

- $\mathbf{X}$ is P times larger
- Iterative solve with the P 2D $\mathbf{L}$ $\mathbf{U}$ factors used as preconditioners
- Uses most of same coding as in linear mode
- Good parallel scaling

3D Nonlinear Solver Strategy

- In 2D, solve efficiently with direct solver up to $(200)^2$ nodes
- In 3D, leads to block triangular structure

$$\begin{bmatrix} \mathbf{B}_1 & \mathbf{C}_1 & & & & & \\ \bullet & \bullet & \bullet & & & & \\ & \bullet & \bullet & \bullet & & & \\ & & \mathbf{A}_j & \mathbf{B}_j & \mathbf{C}_j & & \\ & & & \bullet & \bullet & \bullet & \\ & & & & \bullet & \bullet & \bullet \\ & & & & & \bullet & \bullet \\ \mathbf{C}_N & & & & & \mathbf{A}_N & \mathbf{B}_N \end{bmatrix} \begin{bmatrix} \mathbf{A}_1 \\ \\ \\ \\ \\ \\ \\ \end{bmatrix} \bullet \begin{bmatrix} x_1 \\ . \\ x_{j-1} \\ x_j \\ x_{j+1} \\ . \\ . \\ x_N \end{bmatrix} = \begin{bmatrix} y_1 \\ . \\ y_{j-1} \\ y_j \\ y_{j+1} \\ . \\ . \\ y_N \end{bmatrix}$$

$\mathbf{A}_j, \mathbf{B}_j, \mathbf{C}_j$

are 2D sparse matrices at plane j

Block Jacobi preconditioner corresponds to multiplying each row by $\mathbf{B}_j^{-1}$

PETSc now has the capability of doing this using SuperLU_Dist on each block

Effective “upwind differencing” in pressure equation

- Pressure could become negative during severe events
- In finite differences, it is known that one-sided “upwind differencing” preserves positivity
- One way of viewing this is the diffusive first order truncation error in upwind differencing that is not present in central differencing
- We have added this diffusive term to the finite element equations:

$$\frac{\partial p}{\partial t} = \cdots + \frac{1}{2} h \left|\mathbf{V}\right| \nabla^2 p$$

magnitude of the local velocity

local element size

Exploratory studies on "CMOD" equilibria with $q_0<1$ unstable to a resistive (1,1) mode

Poloidal Flux Ψ

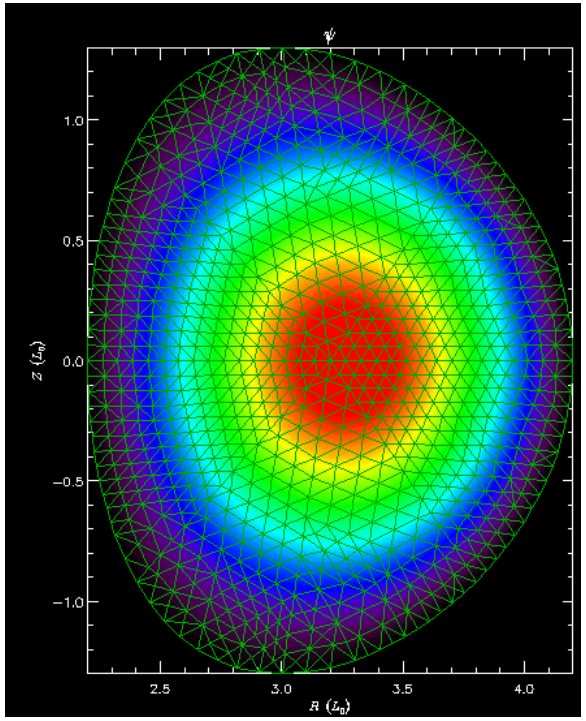

Toroidal Current Jϕ

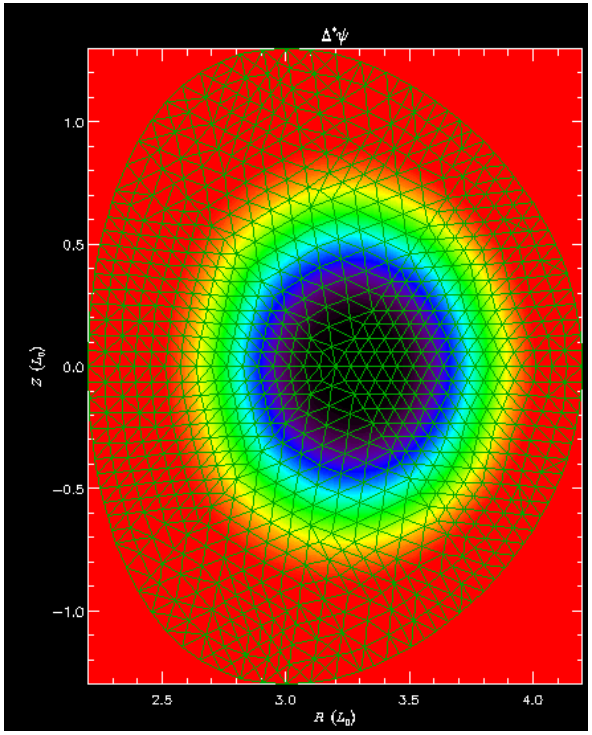

Safety Factor 0.7 < q < 4.5

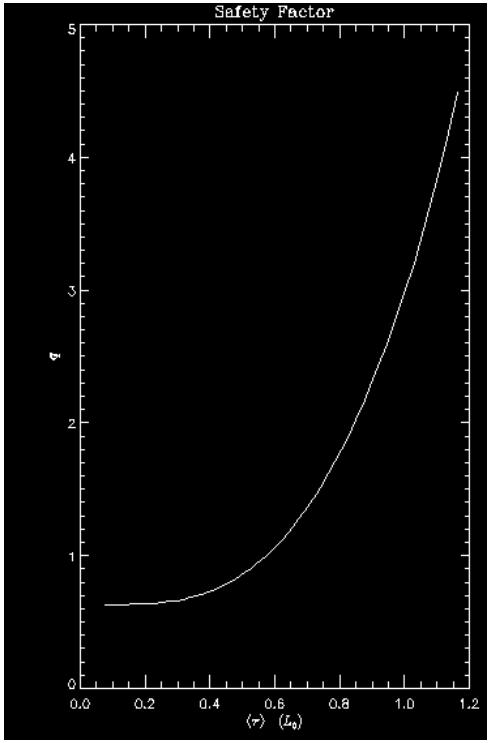

Relatively coarse mesh with ~ 1000 nodes per plane, 8-16 planes.
Initial runs have spatially constant resistivity, viscosity, thermal conductivity, and have initial equilibrium subtracted out with no equilibrium flow.

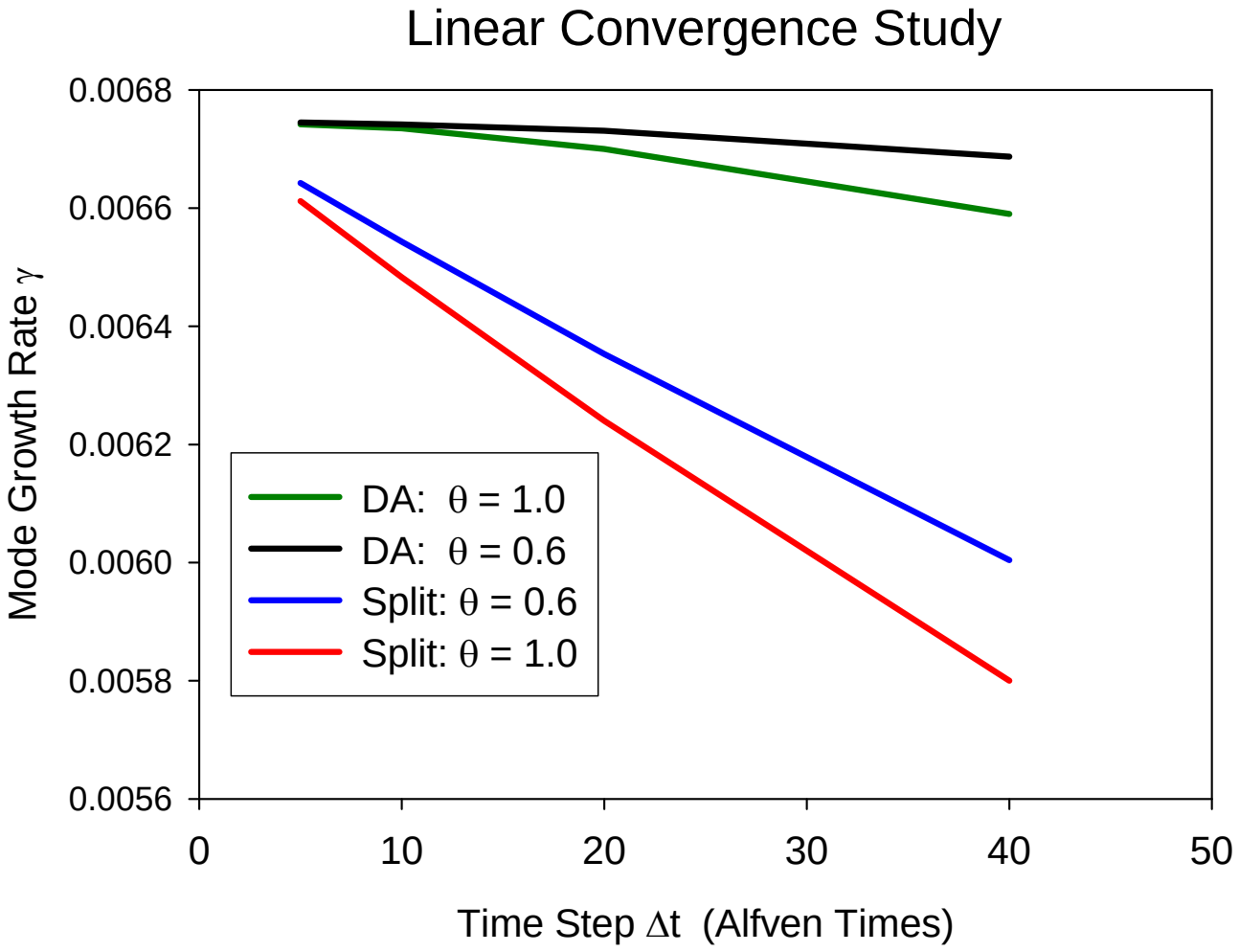

All the calculations are converging to the same point, but the DA (or Caramana) method converges quadraticly and θ=0.6 is best

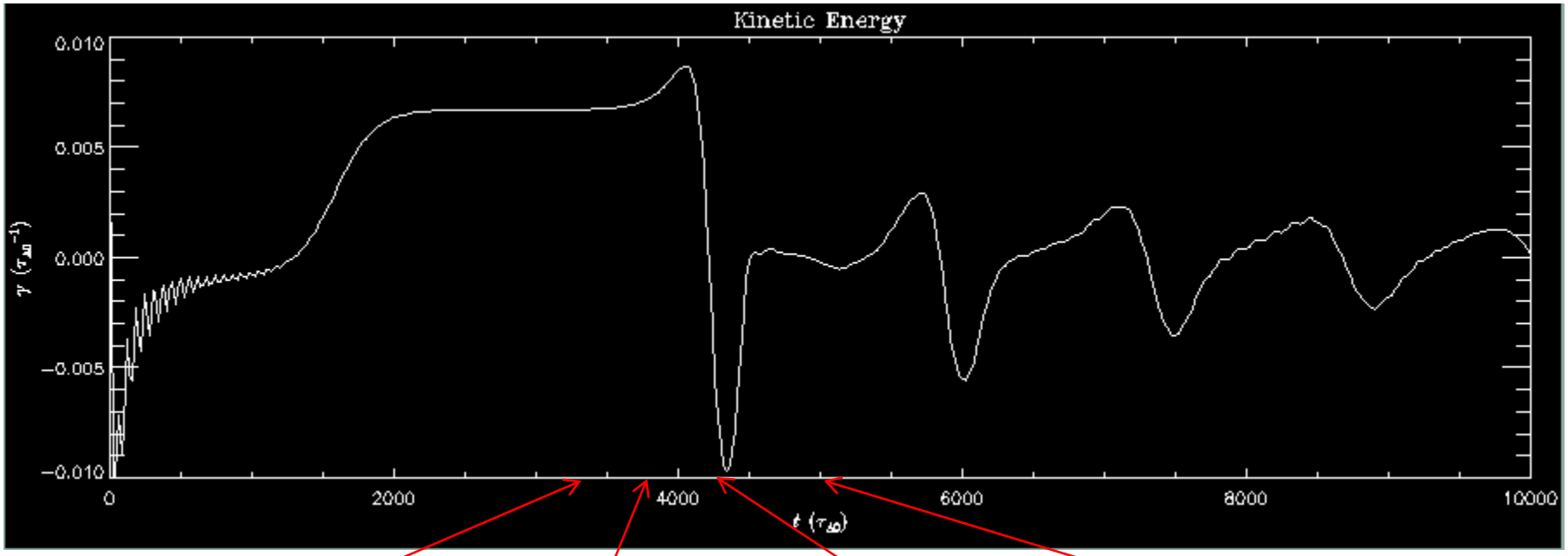

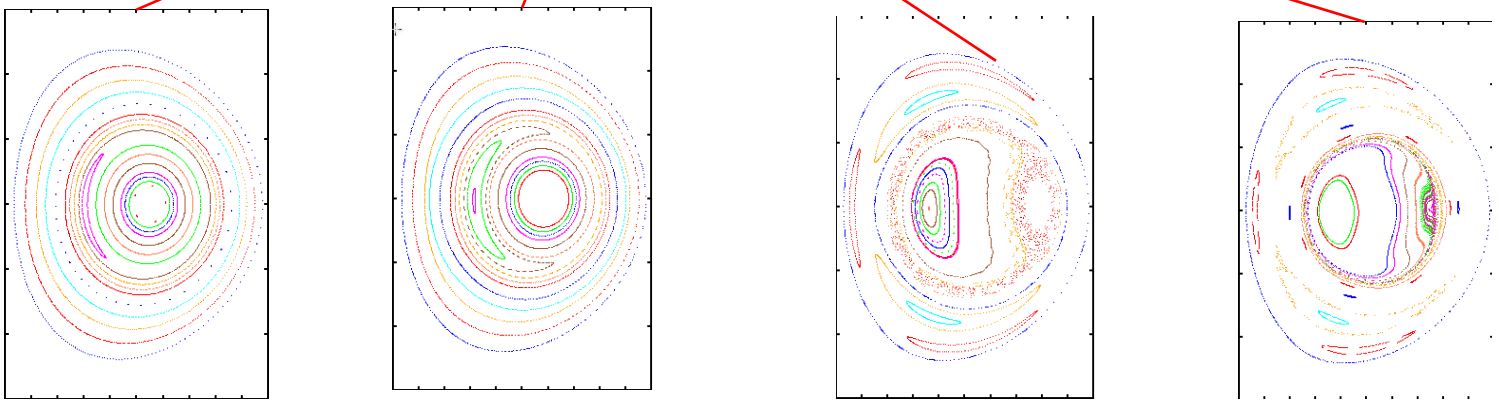

Calculation has long initial linear growth phase, then main reconnection event, then a series of smaller events

Growth rates vs. time for linear, 8 plane nonlinear, and 16 plane nonlinear
Shows nonlinear growth rate is correct and good convergence in # of planes.

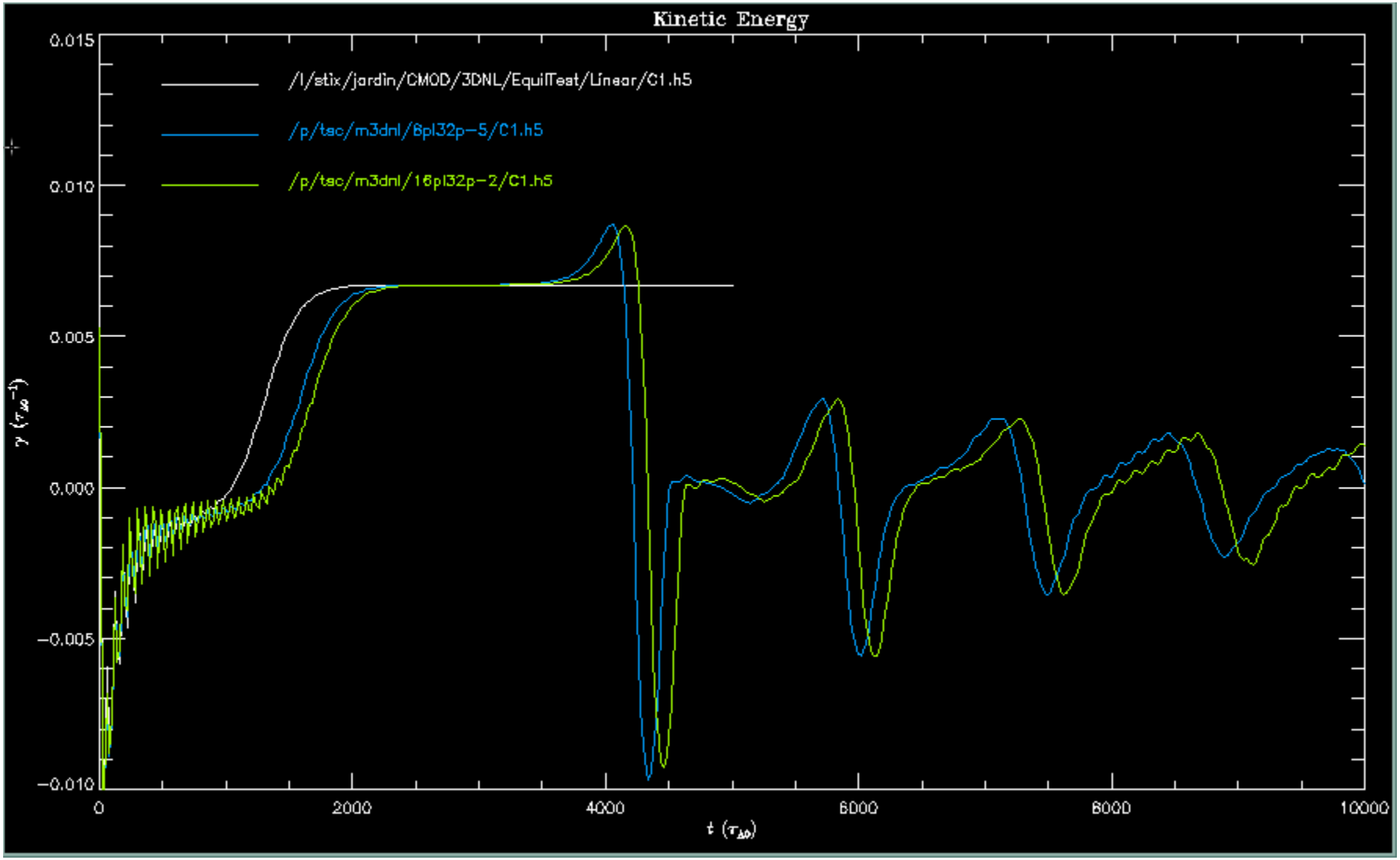

$$\mathbf{V} = R^2 \nabla U \times \nabla \phi + R^2 \omega \nabla \phi + \frac{1}{R^2} \nabla_\perp \chi$$

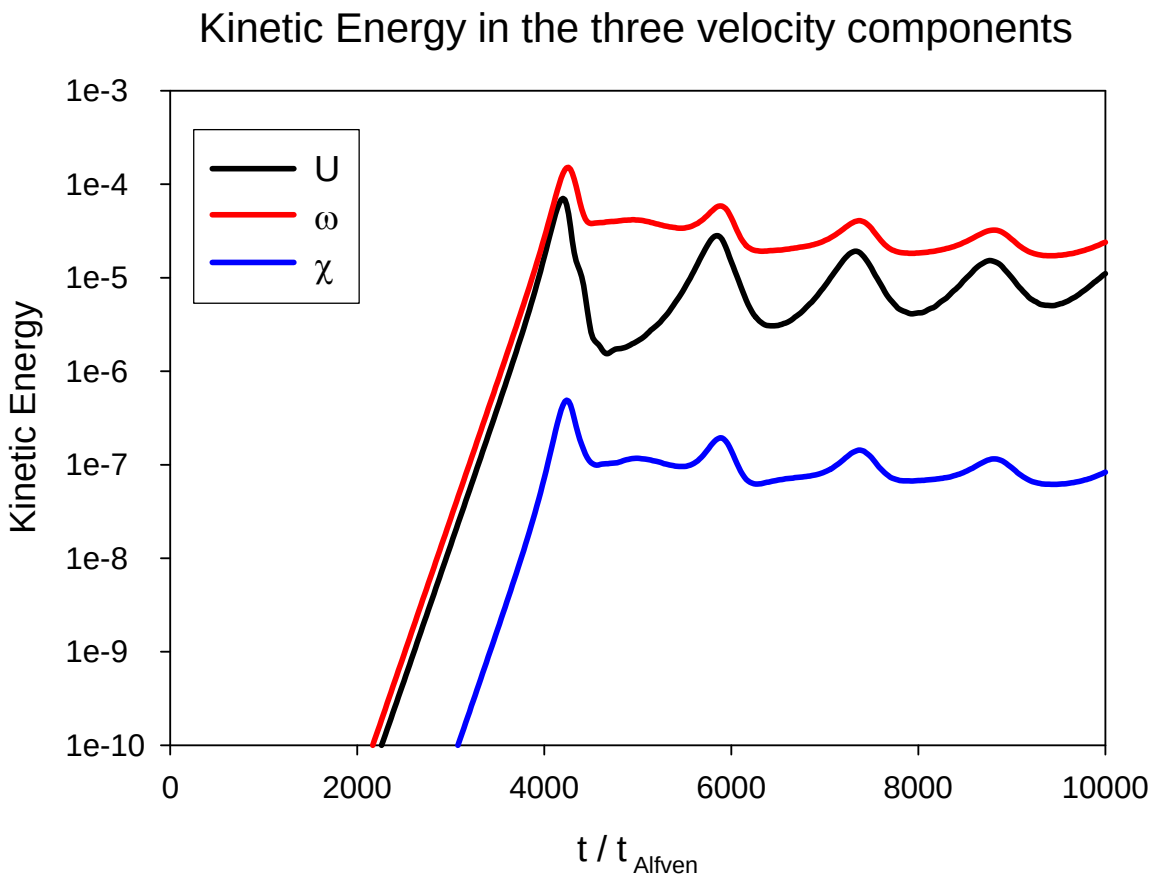

The poloidal velocity decomposition used in M3D-*C*^{1} is very effective in capturing most of the poloidal flow in U.

Kinetic energy, KE, and growth rate ,log(KE), for 20,000 τ_A **θ=1.0**
shows same basic behavior but stronger damping for θ=1 **θ=0.6**

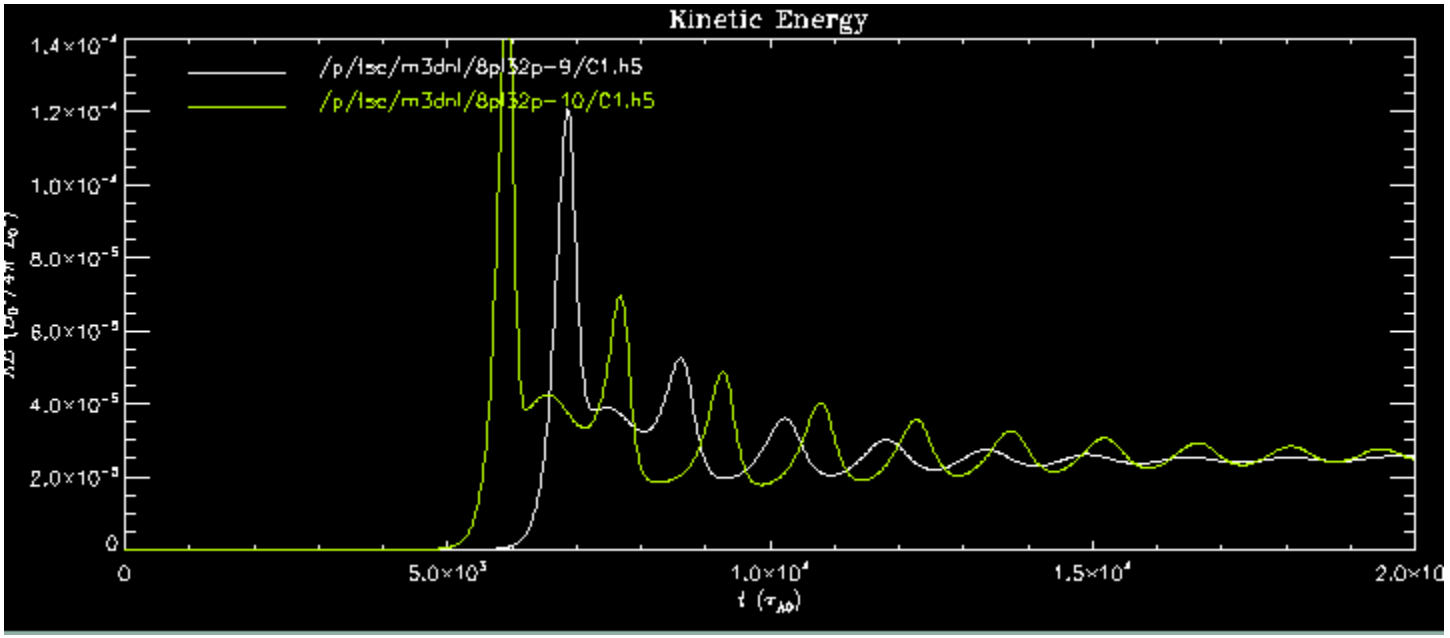

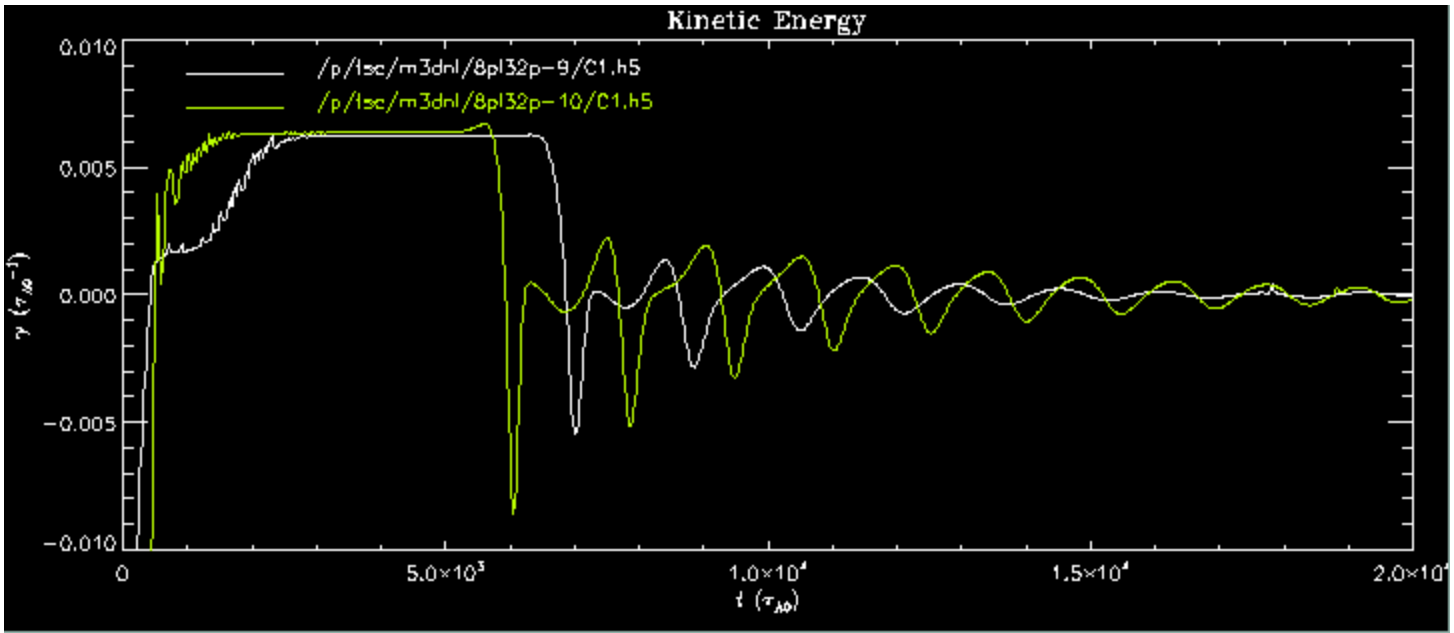

Pressure and toroidal current density do not completely re-symmetrize at t=20,000 τ_A

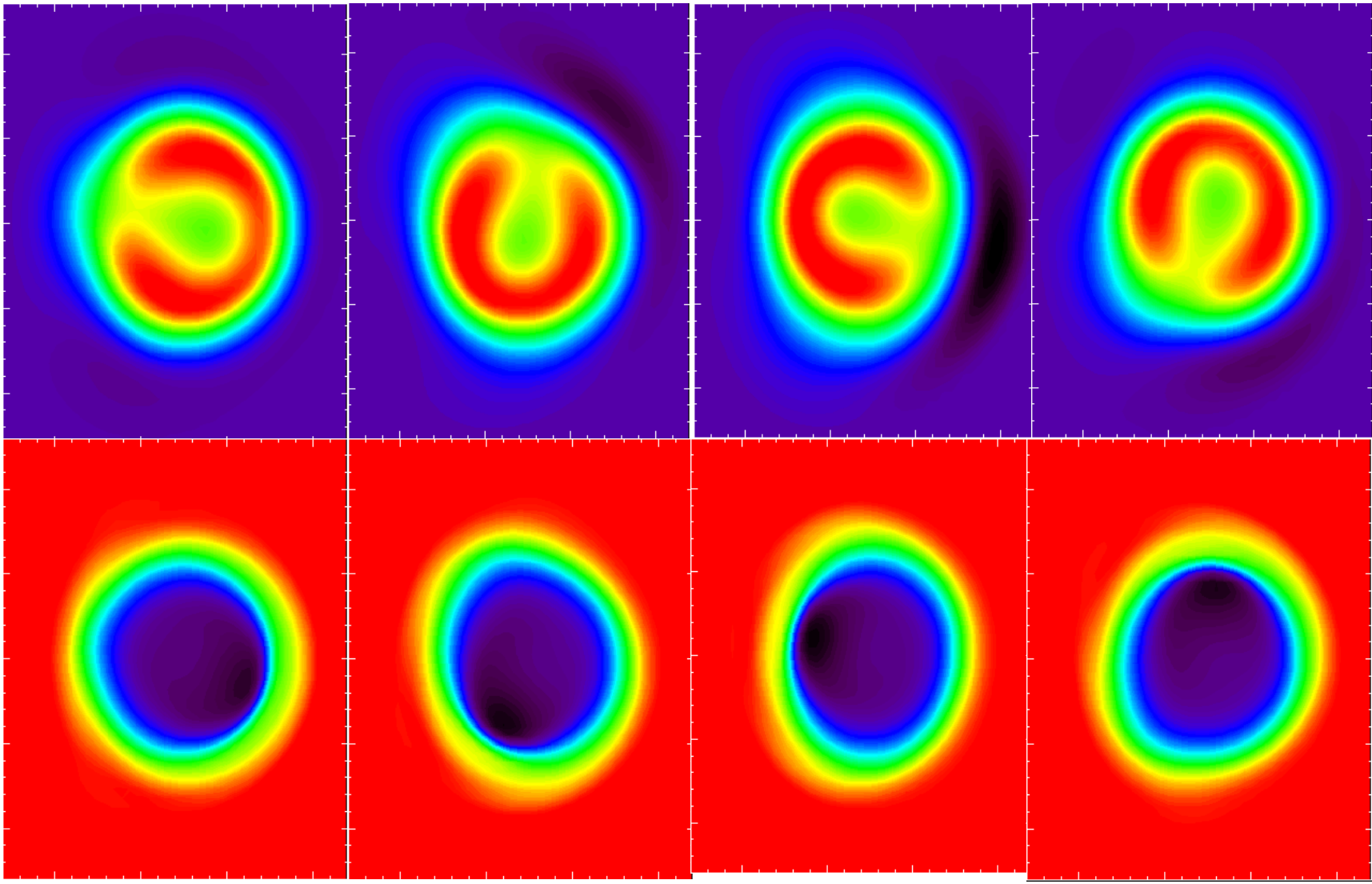

Poincare plot after 20,000 τ_A

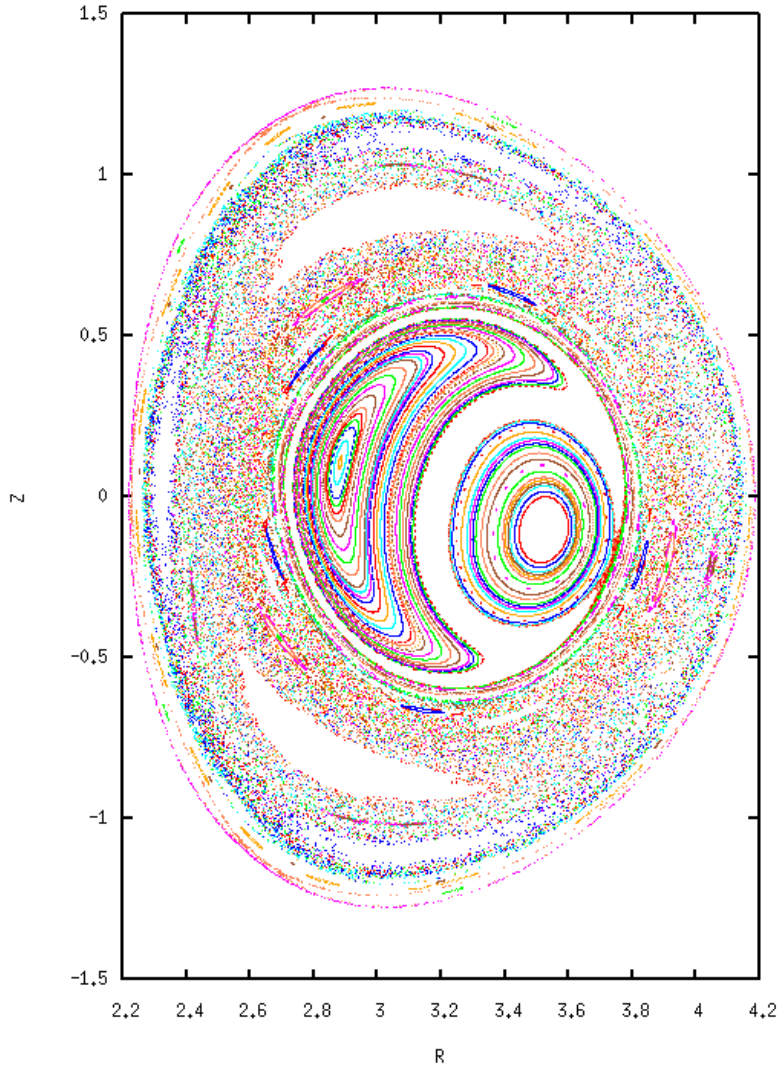

Shows a stationary 3D equilibrium with two magnetic axis.

Postulate that lack of repeated sawteeth is due to the fact that the resistivity and other transport coefficients are constant.

Corrected in the next set of calculations.

Calculations including Equilibrium

In the calculations presented so far, we have subtracted the equilibrium quantities from all variables and assumed that a static initial equilibrium exists with no flow.

$$\psi = \psi_0 + \psi_1 \qquad U_0 = \omega_0 = \chi_0 = 0$$

$$F = F_0 + F_1 \qquad \mathbf{E} + \mathbf{V} \times \mathbf{B} = \eta \mathbf{J}_1$$

The actual equilibrium in a resistive plasma will have flows that will influence the stability. To better represent a real tokamak, we started a series of runs in which the equilibrium is not subtracted.

Also:

- Loop voltage applied to fix total current
- Spitzer resistivity
- isotropic thermal conductivity ~ 1/T

- In 2D (axisymmetry), current continues to peak and q_0 continues to drop with these parameters.

Time evolution with and without equilibrium subtracted off is very different!

Growth rate

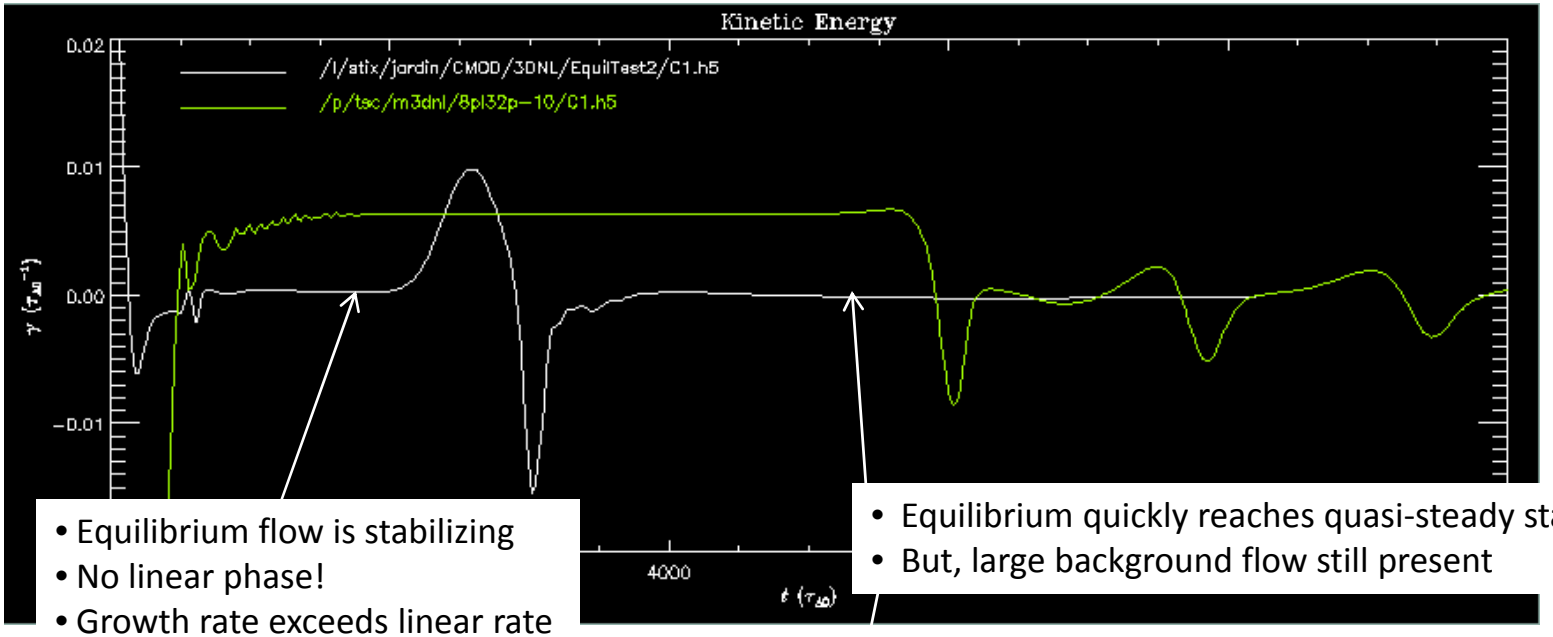

- Equilibrium flow is stabilizing
- No linear phase!
- Growth rate exceeds linear rate

- Equilibrium quickly reaches quasi-steady state
- But, large background flow still present

Kinetic Energy

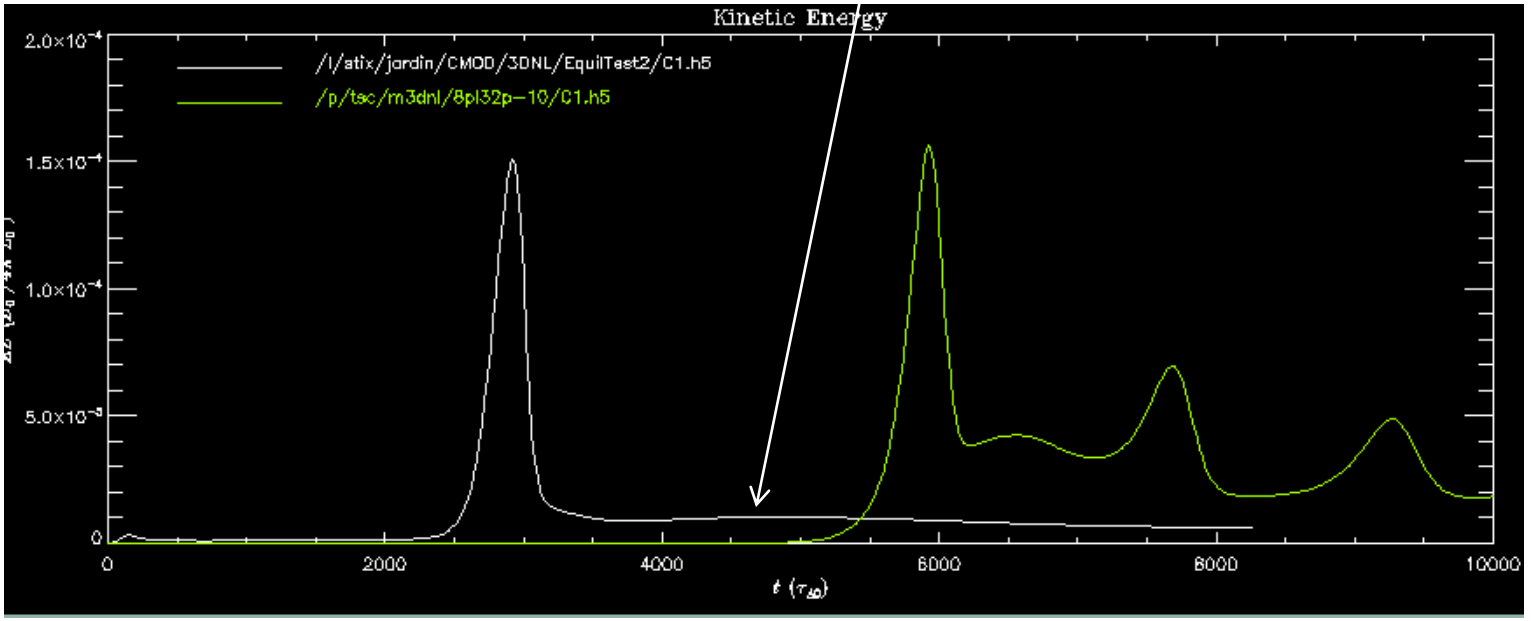

2-D slices of pressure and current density at final time shows non-axisymmetry

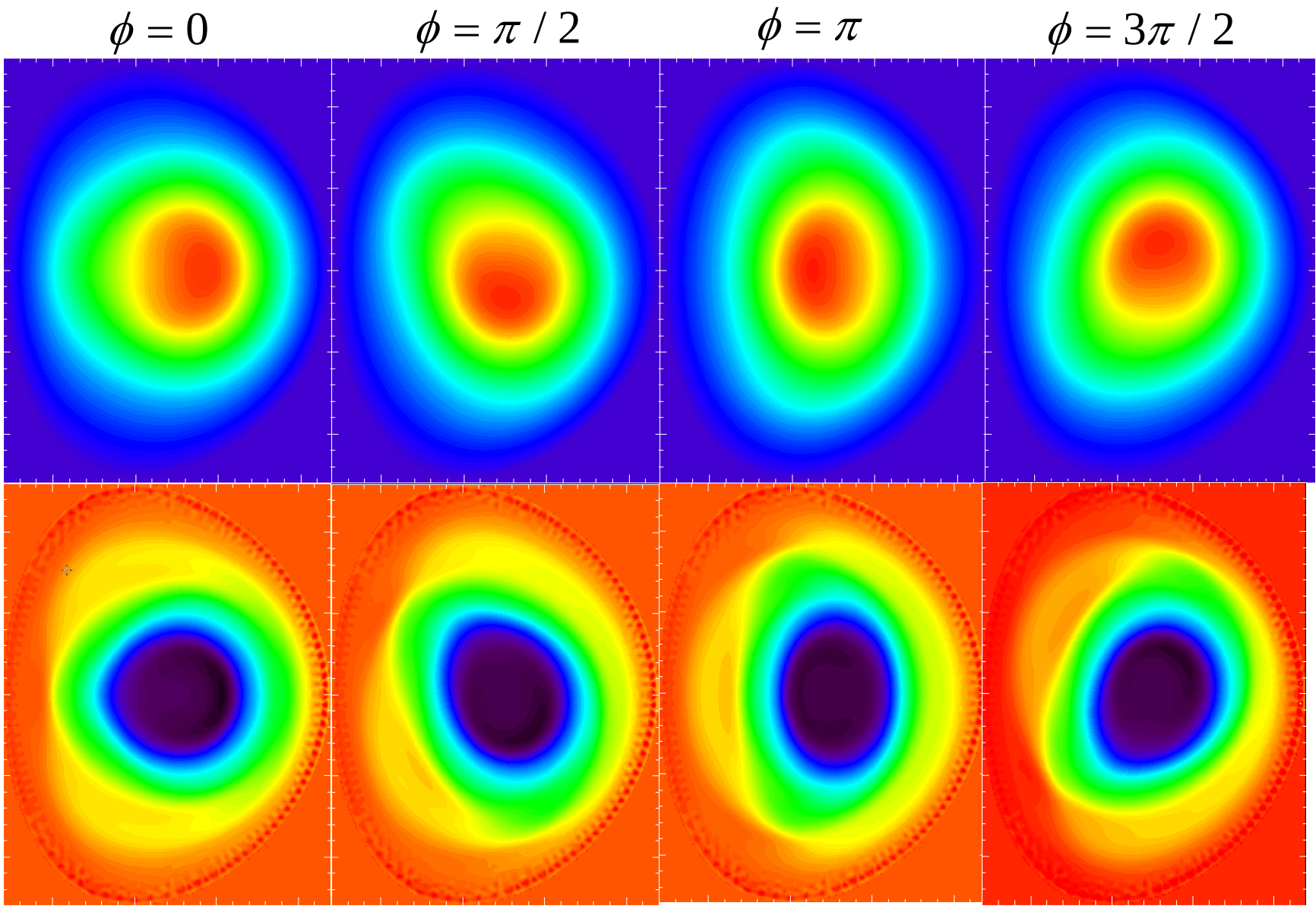

8pl64p-4 slice 95

Stationary flows that exist at the final time in the 3D equilibrium.

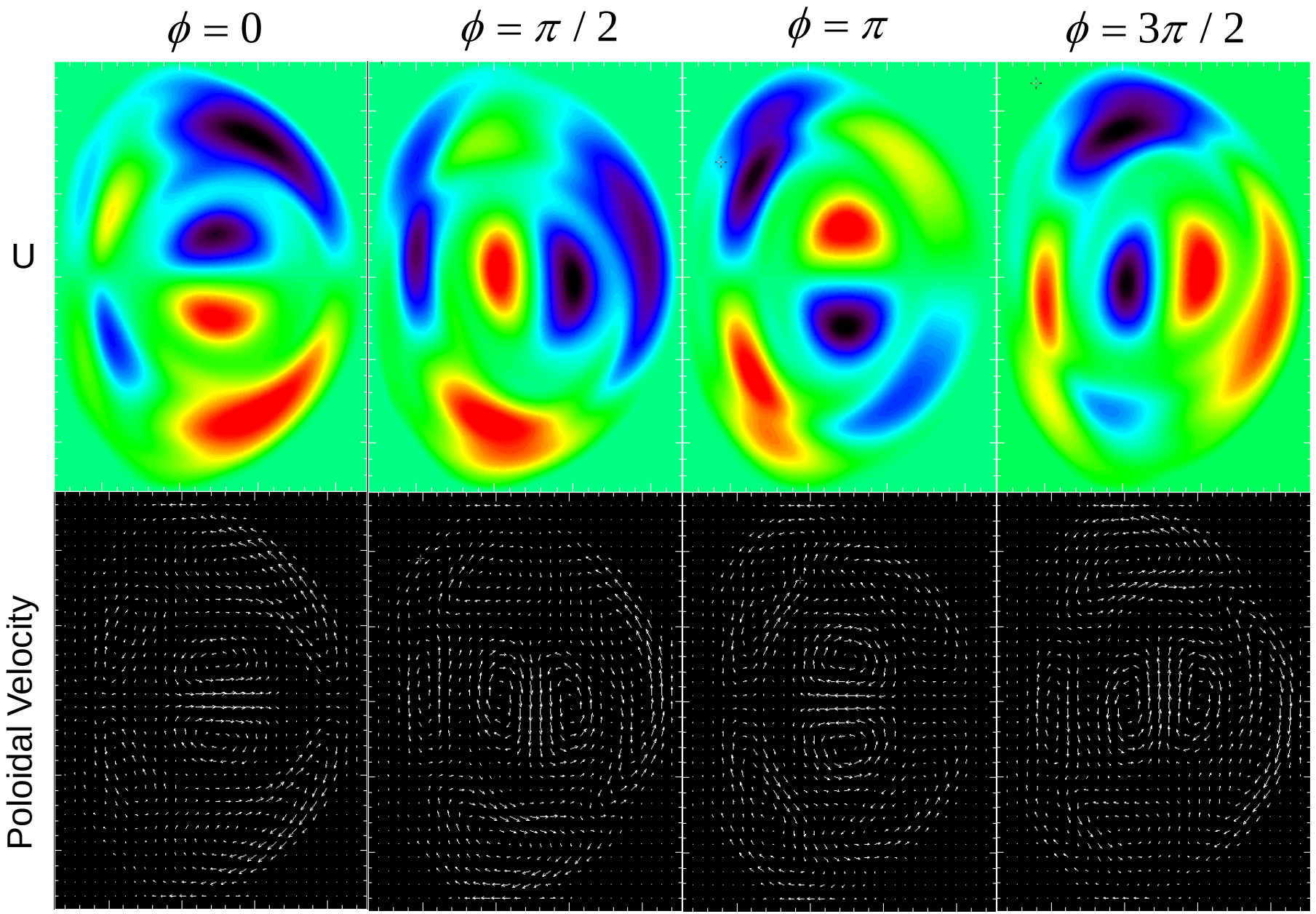

Stationary non-axisymmetric equilibrium with q_0 >1 at t=20,000 τ_A

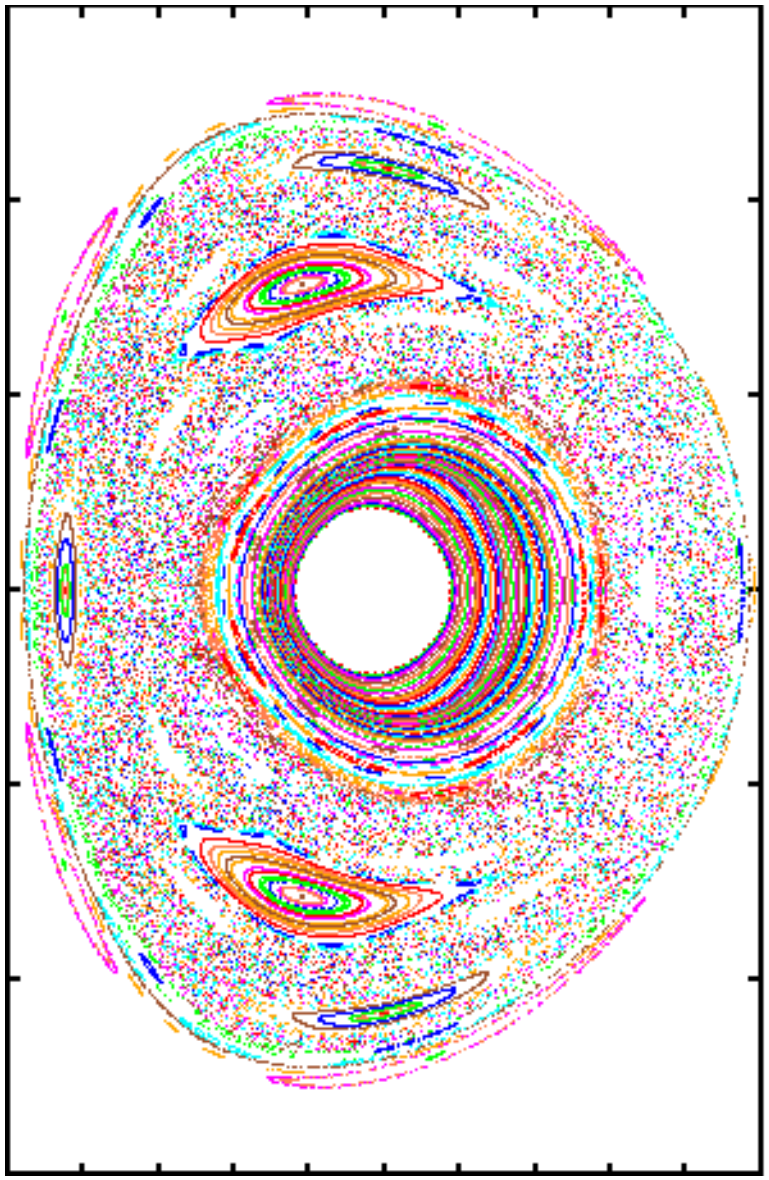

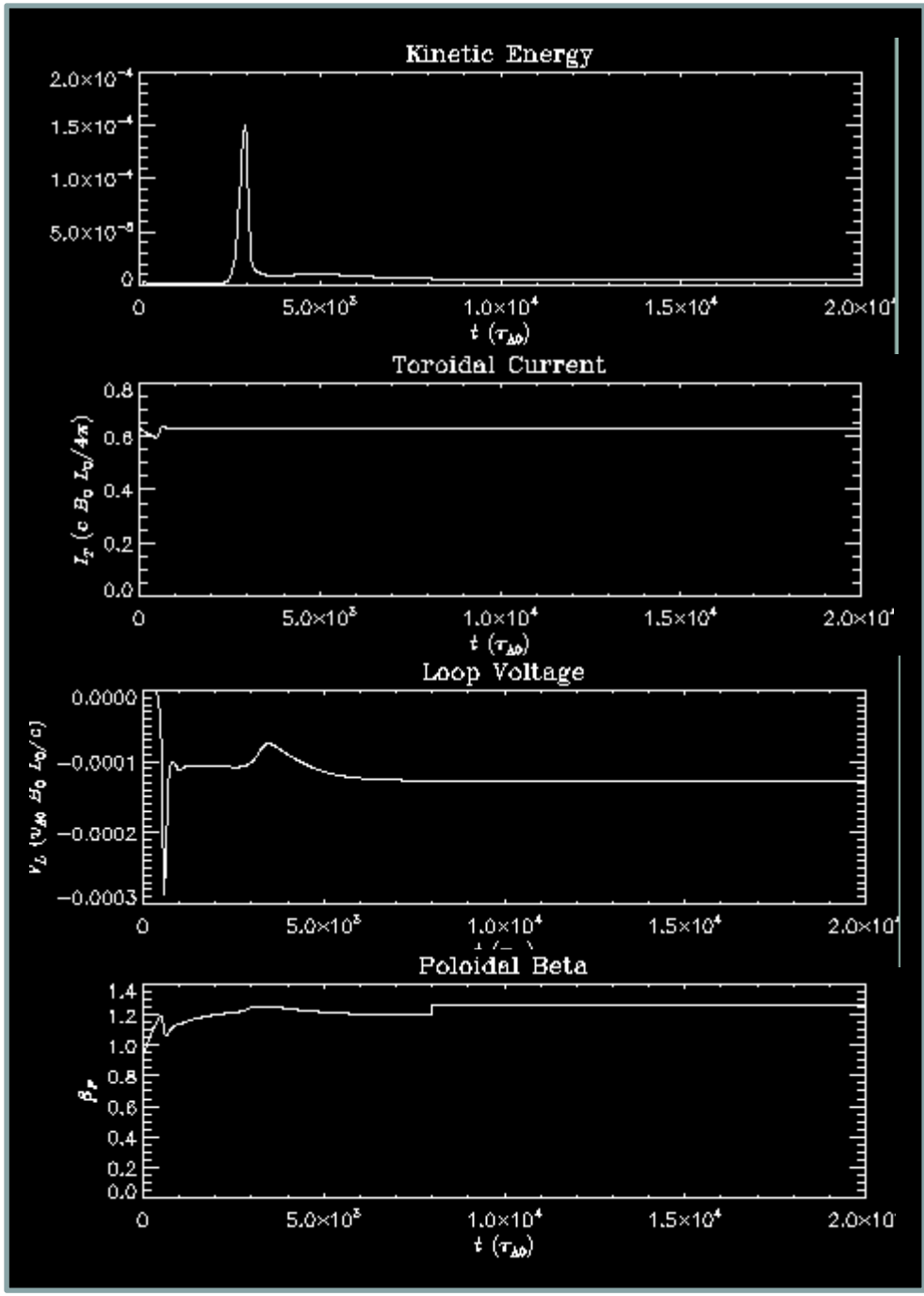

Near Term Physics Studies (extensions)

- Dependence of sequence on transport parameters
  - resistivity,
  - cross-field thermal conductivity,
  - parallel thermal conductivity,
  - viscosity
- Convergence study
  - number of planes
  - number of elements per plane
- Can we get recurring sawteeth to occur for some parameters?
- Inclusion of two-fluid terms in study

Memory Considerations

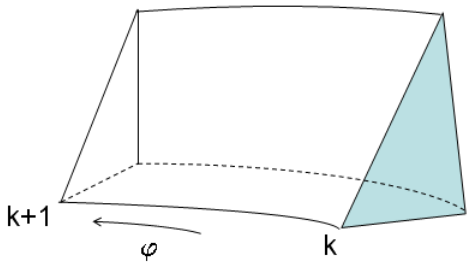

M nodes in each 2D Plane
P Planes (or blocks)

12 unknowns for each scalar for each node
 NV scalars in largest matrix (1, 2, or 3)

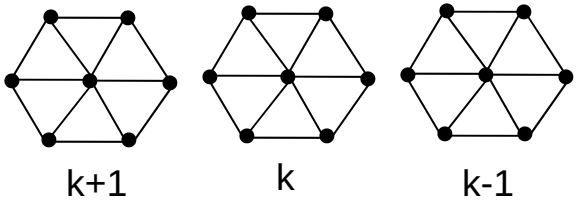

N = 12 x NV x M x P unknowns (or DOF)

Each node is coupled to 21 other nodes via the integrations: k-1, k, k+1

Each matrix row has 21 x 12 x N V = 252 x NV nonzero elements

N rows ➔ 3024 x NV^2 x M x P = nonzero elements

P matrices given to SuperLU

- each with 12 x NV x M Rows, 1008 x NV^2 x M non-zero elements
- LU filling factor of 4 ➔ 4032 x NV^2 x M x P non-zero elements in LU

Each SCOREC word = 14 Bytes….each PETSc word = 25 Bytes

Memory Requirements for largest matrix. Actual memory requirement for code may be twice this.

NV	Nodes / Plane	Planes	NNZ	SCOREC GBYTES	PETSC GBYTES	LU-NNZ (FF = 4)	PETSC GBYTES	Total GB	Hopper Nodes	Hopper Cores
2	107	4	5177088	0.07248	0.12943	6902784	0.17257	0.37448	0.00585	0.14043
3	1000	8	2.2E+08	3.04819	5.4432	2.9E+08	7.2576	15.749	0.24608	5.90587
3	1000	32	8.7E+08	12.1928	21.7728	1.16E+09	29.0304	62.996	0.98431	23.6235
3	4000	64	7E+09	97.5421	174.182	9.29E+09	232.243	503.968	7.8745	188.988
3	16000	128	5.6E+10	780.337	1393.46	7.43E+10	1857.95	4031.74	62.996	1511.9

Future Computational Directions

- Need to get code fully operational on Hopper
- Separate LU decomposition for each velocity component for the Block Jacobi preconditioner
- Multigrid in toroidal direction ?
- GPUs